EVALUATION OF ACUTE AND CHRONIC LESIONS IN PERCUTANEOUS CORONARY INTERVENTION

A Thesis

by

AARON WHEELER ROBERTS

Submitted to the Office of Graduate Studies of
Texas A&M University
in partial fulfillment of the requirements for the degree of

MASTER OF SCIENCE

August 2012

Major Subject: Biomedical Sciences

Evaluation of Acute and Chronic Lesions in Percutaneous Coronary Intervention

Copyright 2012 Aaron Wheeler Roberts

EVALUATION OF ACUTE AND CHRONIC LESIONS IN PERCUTANEOUS CORONARY INTERVENTION

A Thesis

by

AARON WHEELER ROBERTS

Submitted to the Office of Graduate Studies of
Texas A&M University
in partial fulfillment of the requirements for the degree of

MASTER OF SCIENCE

Approved by:

Chair of Committee,	Fred J. Clubb Jr.
Committee Members,	L. Maximilian Buja
	James E. Moore Jr.
Head of Department,	Linda Logan

August 2012

Major Subject: Biomedical Sciences

ABSTRACT

Evaluation of Acute and Chronic Lesions

in Percutaneous Coronary Intervention.

(August 2012)

Aaron Wheeler Roberts, B.S., Texas A&M University

Chair of Advisory Committee: Dr. Fred J. Clubb Jr.

Metallic implants called stents are an important part of the treatment of coronary heart disease. While clinical trials are excellent indicators of outcomes, microscopic evaluation of the host tissue response to the implant is required to assess their safety and efficacy. However, the evaluation of human autopsy tissue containing metal implants presents unique challenges in order to obtain the best results. We used integrated microscopy techniques incorporating microCT and novel plastic histology techniques to demonstrate its effectiveness on human stented vessels obtained at autopsy.

A total of seven cases are demonstrated where our analysis techniques were able to elucidate the pathogenesis of the host response and identify the specific cause of the complications with the stented vessel seen clinically. These techniques are more cost effective and efficient than other techniques currently in use, which could enable them to be used as part of routine autopsy evaluation. The expansion of the pool of stented vessels able to be analyzed to include the often overlooked large population of autopsy cases could provide an enormous amount of data to guide future clinical trials and improve patient care.

ACKNOWLEDGEMENTS

I would like to thank my committee chair, Dr. Clubb, and my committee members, Dr. Buja, and Dr. Moore, for their guidance and support throughout the course of this research.

Thanks also go to my friends and colleagues at the Cardiovascular Pathology Laboratory and the department faculty and staff for making my time at Texas A&M University a great experience. I want to especially extend my gratitude to Stephen Darrouzet, Trevor Lancon, Daniel Grunden, and Erica Moore for assisting me with microCT scanning.

NOMENCLATURE

BMS	Bare Metal Stent
DES	Drug Eluting Stent
MicroCT	Micro Computer Tomography

TABLE OF CONTENTS

Page

ABSTRACT iii

ACKNOWLEDGEMENTS iv

NOMENCLATURE v

TABLE OF CONTENTS vi

LIST OF FIGURES viii

LIST OF TABLES ix

1. INTRODUCTION 1

2. LITERATURE REVIEW 4

    Use of Stents 4
    Testing Stents 4
    Human and Animal Trials 5
    Next Generation Drug-Eluting Stents 7
    Micro Computed Tomography 8
    Histology 9

3. METHODS 11

    Human Autopsy Specimens 11
    High Resolution Digital Photography 11
    MicroCT Analysis 13
    Histology 13
    Digital Slide Imaging 13

4. RESULTS 15

    Case 1: Ruptured Soft Plaque 15
    Case 2: Acute Dissection 17
    Case 3: Vulnerable Plaque Erosion and Thrombosis 19
    Case 4: Mural Thrombus 22

Page

Case 5: Overexpansion Contralateral to a Hard Plaque 24
Case 6: Long-Term Drug Eluting Stent 29
Case 7: Complex Multiple Implantation 32

5. DISCUSSION AND CONCLUSIONS 38

REFERENCES 41

VITA 46

LIST OF FIGURES

FIGURE		Page
1	Vulnerable Plaque Rupture	16
2	Calcified Plaque Dissection	18
3	Effects of No Antiplatelet Therapy	21
4	Mural Thrombus Dissection	23
5	Over-Expanded Strut Contralateral to a Calcified Plaque	25
6	Internal Elastic Lamina Rupture Site	26
7	Distal Rupture Site	28
8	Proximal Drug-Eluting Stent	30
9	Distal Drug Eluting Stent	31
10	Subgross Sectioning Overview	34
11	Specific Findings	36

LIST OF TABLES

TABLE Page

1 Summary of Evaluated Cases..... 12

1. INTRODUCTION

Since their introduction in the 1980s coronary stents have evolved into a widely used treatment for occlusive artery disease in the United States, with > 650,000 implantations performed each year(1). However, the use of coronary stents has recently come under scrutiny as to whether they are any more effective than pharmaceutical intervention in chronic cases (2,3). The routine evaluation of these devices is often limited to clinical observations and coronary angiography because of the inherent drawbacks of traditional processing techniques for postmortem specimens. Clinical trials excel in their ability to present strong statistical data on the clinical outcomes of these kinds of therapies. But they fall short when describing the mechanisms of the disease process. It is in this regard that autopsy evaluation of tissues is "uniquely capable of providing information regarding the pathobiological phenomena that predispose those patients to good and adverse clinical outcomes"(4).

Stented coronary artery tissue obtained at autopsy provides a valuable look at both the pathology of the vessel and the mechanical properties of the implanted stent (5). However, the available techniques for the histological evaluation of these tissues and stents are limited in both results and efficiency that may hinder their use in the regular evaluation for research studies. Paraffin embedding, the standard for histological processing, fails due to the compliance mismatch between the metal device and the surrounding tissue. During routine sectioning, the sample may collapse and become irrevocably damaged.

The need to analyze autopsy specimens in the most efficient way possible comes from a growing need for human pathology data, especially when discussing "off-label" use of

---

This thesis follows the style of The Journal of the American College of Cardiology.

stents (6). Current animal trials for stents only evaluate the “on-label” use guidelines for the devices that are generally narrow and don’t represent all conditions that a stent may be implanted in (7,8).

Choosing a methodology to evaluate a one-of-a-kind specimen, such as those obtained at autopsy, can be a challenge. This is especially true when analysis techniques are mutually exclusive or destructive to the sample. Therefore targeted and precise analysis techniques that incorporate several methodologies onto the same specimen become quite valuable to the researcher or clinician.

Plastic embedding in different types of resins have shown to be effective in maintaining varying degrees of tissue morphology(9,10). These plastic embedding techniques are expensive and time-consuming when performed with traditional serial sectioning methods and cause a loss of specimen tissue during processing. When processing valuable specimens, inadvertent destruction of diagnostically important areas of the vessel is always a risk. Micro-CT, with a resolution of 13 micrometers, is capable of identifying gross flaws in stent structure and deployment. And using the reconstructed three-dimensional volume, occlusions, restenosis, calcific plaque formation, and other forms of vascular damage can be located(11). Micro-CT scanning can guide histology sectioning towards areas of interest to produce precise representative sections that do not cause collateral loss of tissue. These targeted sections can be compared to the entire three-dimensional volume to obtain more information about the overall topography of the vessel lesions and validate the microCT measurements.

We hypothesize that integrated microscopy techniques will reduce turnaround time and tissue loss because sections can be extracted from specific areas without serially grinding or cutting through the entire specimen. High-resolution sections enable pathologists to gain more information from a single specimen and therefore learn more from individual specimens and reduce waste in the evaluation process. With an

expanded set of methodologies and protocols, tissue obtained at autopsy could be used more extensively to assess the efficacy of coronary stents. This will have both the advantages of increasing efficiency compared to traditional, time-consuming serial sectioning, and also allow cross validation of microCT findings with direct histological evidence in order to provide new data on the performance of stents from an often overlooked source.

2. LITERATURE REVIEW

Use of Stents

The demands for more robust evaluation of stents and PCI come from recent studies that call into question the appropriateness of PCI in treating patients with certain types of coronary heart disease. The most recent study of the appropriateness of PCI, done in 2011, was a clinical outcomes evaluation of a large cohort of patients (500,154) over several years. The study found that the use of stents was deemed inappropriate for 12% of non-acute indications, and appropriate for only 50-58% for non-acute indications(3). All acute case indications were deemed appropriate. These trends are difficult to explain when the primary labeled and FDA-approved use of stents is for stable patients with chronic angina and no other medical complications until one considers that more than 60% of stent use is off-label (2). Chan and his colleagues were careful to stress the value of expanding the testing practices for both the pre-clinical and clinical phase of stent development, as well as post market surveillance of off-label use (3).

Testing Stents

A perfect example of the need of a more directed and inclusive testing paradigm is that of the development and use of drug eluting stents over the past two decades. Medical devices require only minimal testing in the United States in the pre-clinical and clinical phases because of the 510(k) route where the existence of a predicate device can be used as evidence of the effectiveness of the newly developed device. In short, stent companies can submit past evidence of the effectiveness of a device as evidence for a new device as long as there are reasonable similarities. This allowed the first generation of drug eluting stents, in particular: which are the combination of predicate bare metal stent designs and already proven anti-neoplastic drugs, to be brought to market much faster than other types of medicine. The FDA still required long-term surveillance of clinical trial patients (up to 5 years(2)) and an adequate study size to produce valid conclusions(4,12-16), but flaws in the study design can be seen in hindsight.

In a 2005 report of the incidence and predictors of thrombosis in DES, Iakovou and colleagues found increased incidence of in-stent thrombosis in "real world" patients 9 months after implantation, significantly higher than what was seen in patients during clinical trials(17). Their explanation was that physicians had been discontinuing antiplatelet therapy in "real world" patients in the wake of observations of significantly less in-stent restenosis in those patients. Until then bare metal stents were producing high levels of in-stent restenosis, and anti-platelet therapy was important because a narrower lumen was more susceptible to occlusion. The physicians had no idea of the danger late thrombosis posed to DES implants, and were only trying to minimize the negative effects of dual antiplatelet therapies, which are not always well tolerated in some patients. Patients enrolled in the original clinical trials were all required to continue dual anti-platelet therapy for the course of the trial(17).

Human and Animal Trials

Following the growing concern over late in-stent thrombosis, animal trials were revisited in order to uncover an explanation. In 2007 Nakazawa's group suggested why the late effects of DES implants were overlooked in animal trials. They showed that while pig and rabbit models were adequate for mechanical testing of coronary stents, the rates of re-endothelialization are not quite as close to those seen in humans, who take much longer to re-endothelialize. This discrepancy was such that the pre-clinical testing window of 90-180 days showed successful, albeit delayed, endothelialization of the lumen of the stented vessel in porcine models. However when tested in humans the delayed healing process can take almost a year or more to reproduce the same results(18). So when the same time points that were used to test successful endothelialization in animals were applied to recommendations for the discontinuation of anti-platelet therapy in human patients, DES use led to complications in "real world" use. Nakazawa et al. claimed that if the results of animal trials had been interpreted

correctly and properly scaled to human healing time points, complications in clinical use could have been predicted.

Our understanding of the pathology of stented lesions is constantly advancing but is based on a key idea: the implantation of a device in the artery will elicit a response from the body. It is the type and cause of the response that is steadily becoming better understood. The vessel response to injury from an angioplasty balloon was described in 1987, when it was observed that endothelial disruption would lead to thrombosis in the injured artery(19). Later, in 1992, another group described their findings in a porcine model at 4 weeks after implantation that the rate of restenosis was proportional to the amount of medial injury from overexpansion of the vessel wall(20). An important distinction must be made between observations in porcine arteries and human arteries; because they do behave differently than human arteries. Porcine arteries endothelialize and recover from injury much faster(21), but more importantly they are not often diseased when used for testing of stent implants(22). And those conclusions drawn from porcine studies should be compared to equally rigorous studies in diseased human arteries containing plaques. In 1999 Farb et al. described the differences in the pathology of human stented lesions, compared to porcine models, and concluded that while most injury in human implants is associated with the plaque, porcine injury often involves the media directly(23). Furthermore the rapid re-endothelialiation of the pig sequesters fibrin around the struts of the stent, limiting their exposure to the lumen and possibly limiting thrombosis in pigs(22).

Another study in 2006 by Joner and colleagues again confirmed that human arteries endothelialize slower than porcine arteries(21). In addition, they confirmed that first generation drug eluting stents in humans show delayed healing and hypothesized that the delayed healing process places vulnerable lipid plaques at risk of rupture and exposure of thrombogenic material to the lumen(21). That same year another group showed that prolonged damage to the endothelium or other limits to healing leads to increased

frequency of thrombus formation on its own, even when patients were on dual anti-platelet therapy(15). To try and uncover the mechanism of thrombus formation, a study was done in 2007 using atherectomy to identify the type of material in the vessel wall that was initiating a thrombogenic response. They found an incomplete neointima over two years after implantation (24,25). Because the endothelium of the vessel wall remained unhealed, the inflammatory and thrombogenic pathways were at risk of being triggered even at long-term time points (26). Because of this van Beusekom and colleagues advocated extending dual antiplatelet therapy for patients already implanted with DES, and the deployment of long term studies that correlate both histology and imaging to better understand the mechanisms behind late thrombosis.

Next Generation Drug-Eluting Stents

The second and third generation of drug eluting stents, currently being developed and tested, were inspired by several studies that demonstrated a link between restenosis, neo-intima plaque formation, and the inflammatory response(5,27,28). In 2002 Farb's group commented on how, even though the first generation of DES using anti neoplastic agents to suppress smooth muscle cell proliferation were successful, the addition of anti-inflammatory drugs might help further temper the reaction(5). A new model of DES utilizing pimecrolimus in porcine models has shown promising results for decreasing restenosis and late thrombosis (29,30). However long term human trials will be the deciding factor because both the FDA and the scientific community have taken note of the lessons learned from the first generation of DES(13). With over 6 million DES currently implanted in human patients, the need for a direct histopathological evaluation process that can elucidate mechanisms of disease is apparent.(13)

Direct observation of tissue associated with the healing process of stented arteries is crucial to settle the current debate over the nuances of the exact mechanisms of disease and healing. Whereas past studies before 2012 have suggested incomplete endothelialization as the culprit for late in-stent thrombosis, new research is revealing

that it may be more complicated. Recent findings using angioscopic imaging have shown that the degree of neointimal coverage is not related to the prevalence of in-stent thrombosis. Instead, the host reaction is more directly related to the health and type of the endothelium, the type of polymer coating, drug, dose, and other stent characteristics(31). The long-term onset and low frequency of thrombosis also presents a challenge to researchers trying to reliably reproduce lesions for study, especially as current recommendations for long term antiplatelet therapy garnered from first generation DES outcomes would put patients at too much risk to ethically test the effects of dual anti-platelet therapy in clinical trials, a limitation that may confound the results of clinical analyses(32).

Regardless of the concerns for the safety and the future analysis of DES, the technology is a promising and inspired step forward in improving medical implants. Because the high risk of restenosis in BMS outweighs the risk of late thrombosis in DES, there is no difference in mortality from BMS compared to first generation DES as long as patients continue to take long term anti-platelet therapy(33). Of course, the need to find a device that avoids the need for anti-platelet therapy in patients that may not tolerate the treatment due to secondary factors still exists. DES are also the indicated treatment for restenosis of BMS based on clinical outcomes. However all the different factors involved for re-implantation of another stent are not well studied at the microscopic level, and there is limited data regarding the optimal use of DES in such cases(12). Furthermore, DES still require direct pathology observation along with microscopic evaluation and other methodologies in order to confirm the performance of the stent at all levels of testing moving forward(12,34).

Micro Computed Tomography

MicroCT scanning is a robust technology for the evaluation of materials and tissues in three dimensions. The technology using a series of x-ray micrographs that are then reconstructed into a volume by a computer(35). MicroCT was first used for bone and

bone implants, and has been proven to provide good correlation to histology(36). The feasibility of microCT scanning when applied to autopsy specimens of coronary artery wall lesions has been described by Langheinrich et. al. when they analyzed vulnerable plaques and the nature of underlying lesions in acute coronary events(37). They stated in their rationale for the use of microCT that histology on its own is limited as an analysis tool. Their concerns included the expensive and time consuming nature of serial sectioning, the destruction of the tissue that causes it to be excluded from other analysis methods, and the lack of three-dimensional data that precludes longitudinal measurements. The idea of an integrated approach to medical device evaluation that incorporates CT imaging and histology was first described in 2008(38). Jason Foerst demonstrated stent analysis using microCT in 2010 when his group scanned and reconstructed an entire stented vessel from a patient that had received two stents 5 months before death. In their findings they noted the ability of the microCT methodology to reveal fractures in the stent struts as well as the location and morphology of calcified plaques in the vessel wall and along the stent. Their analysis was limited to an evaluation of the performance of the device by observing the fracture patterns(11).

Histology

Histological processing of metal stent implants has come a long way in the last two decades. Originally, struts had to be manually removed from the tissue following fixation but before embedding(39). This process was necessary because tissues are usually embedded in paraffin wax, which does not tolerate the presence of metal in the block. A method of using methyl-methacrylate (MMA) plastic resins was introduced in 1996 that demonstrated the implant could be left in the tissue during processing and then cut on a motor driven rotary microtome(40). The problem with these plastic sections is that they are difficult to stain due in a large part to their hydrophobic nature. Hydrophilic stains are unable to penetrate the hardened plastic matrix, and therefore substitute stains using small molecular weight molecules and non-aqueous solvents were developed(41).

To improve cellular detail and increase the number of available stains for plastic embedded tissues: deplastination techniques were developed. The caveat is that only certain types of plastics could be removed from the section, and they are usually the most volatile, and dangerous to handle(9). In 2006 Peter Rippstein et. al. published a review of the available plastic sectioning techniques to determine which produced the best, most reliable, results(42). In their conclusion they noted that using a microtome produced sections with the most consistent thicknesses. However, the high potential for blade damage due to the dense metal struts could cause unwanted artifact. The alternative is to use a sawing and grinding method (SG), also referred to as microgrinding, which they stated "consistently produces intact specimen sections without displacement of the struts or scoring of the tissue." The drawback is the plastic in SG sections cannot be removed safety because of microscopic scoring lines from the grinding process that fray and produce artifact. Therefore the staining and cell detail seen in SG sections is usually of lower quality. Rippstein's group did, however, discover that using heat during the staining process improves the contrast of the final result(42). One year after their review, a new type of plastic embedding media was invented, called Technovit 7200. This resin is a variant of methyl methacrylate, called isobornyl methacrylate, which is much harder and shrinks less during processing so the architecture of the tissue is much better maintained during processing. Furthermore the resin is a light hardening monomer instead of a catalyzed polymer like MMA, and is much less volatile and dangerous to use. However it is significantly more hydrophobic than MMA and cannot be removed from the section so it is more difficult to stain(43). Other methods of processing metal stent implants that avoid using plastic have been suggested, such as using electrochemical processes to dissolve the stent in a salt acid bath under DC current (44).

3. METHODS

Human Autopsy Specimens

Stented vessels obtained from human patients at autopsy showing signs of severe coronary artery stenosis, calcific plaque formation or coronary artery disease were provided from the Texas Heart Institute (Houston, TX, USA). There were 12 cases in total, 7 of which are presented in this paper because they showed results relevant to the demands of clinical evaluation of stents (Table 1). These cases were analyzed as part of a clinical autopsy evaluation service provided by the Cardiovascular Pathology Laboratory at Texas A&M University. Relevant clinical information was collected where available and patient identities were anonymized. The patients were implanted with metallic stents at varying time points for different durations but all showed complications arising from the stent implantation or the areas related to the implanted stents. The specimens were fixed in 10% neutral buffered formalin at the time of autopsy. All specimens were evaluated according to standard operating procedures developed by the Cardiovascular Pathology Laboratory for the analysis of metal implants. Methodologies used include microCT, with contrast material in the lumen if necessary, and targeted microground histology on areas of interest in the specimen. Specimens were grouped by type of stent and implant duration.

High Resolution Digital Photography

A high-resolution digital single lens reflex camera (Canon Mark 3, Canon Inc., Lake Success NY) was utilized to photograph each specimen from multiple perspectives. Gross features were noted for analysis and the photographs will serve as a record of the gross orientation and appearance of the specimens.

Table 1: Summary of Evaluated Cases

Case #	Case Type	Time	Stent Type	Clinical History	Microscopic Findings
1	Acute	N/A	Liberte Taxus Paciltaxel-Eluting	Stent implanted in the RCA for acute MI. Evidence of eroded plaque with thrombus downstream. No reflow phenomenon.	Eroded/ruptured plaque in the RCA. Unable to tell if it was associated with the procedure.
2		N/A	Medtronik Integrity Bare-Metal	Stent in proximal left main. Presented with acute coronary syndrome	Severe mineralized plaques in a branch artery expanded on implantation and lead to rupture of the vessel wall with concurrent stent fracture.
3		1 wk	Boston Scientific Liberte BMS	Stent in LCX. Presented with multiple healed sub-acute to acute MI, Patient did not take Plavix due to cost issues.	Focal soft plaque rupture and erosion. Evidence of thrombogenesis consistent with clinical signs.
4		N/A	J&J Cordis Cypher Sirolimus-Eluting	Stent placement on admission to L. circumflex obtuse. 10% stenosis post-deployment. Peri-procedural MI.	Stent deployed against a mural thrombus with a thin fibrous cap. Dissections of the cap and rupture of soft plaque.
5	Chronic	2yr	Abbot Multilink Vision Bare-Metal	76 y/o female. Presented with acute coronary syndrome and died after CBG	Focal calcification produced an area of contralateral overexpansion and IEL rupture
6		6yr	J&J Cordis Cypher Sirolimus-Eluting	Male, unknown age. DES implant in LCCA in 2004. Presented with severe CAD.	Interrupted healing of the endothelium and peri-strut region. Exposed struts in the lumen
7		9yr + 2yr	Multiple DES/BMS	History of CAD. >10 stents in the RCA	Neo-intima proliferation in the region of media rupture. In-stent atherosclerosis with mineralization. Degeneration of the media and IEL in the distal RCA.

A total of 7 cases were evaluated using integrated microscopy techniques. The clinical history and indications as well as relevant findings for each case are summarized.

MicroCT Analysis

Samples were scanned using a HAWK-160XI (Nikon, Chiyoda-ku, Tokyo) microCT system. The system uses a cone-beam X-ray detector and source configuration for image acquisition with a tungsten target for generating X-rays up to 160kV. Approximately 1000 projections were completed for each scan with an average of two scans performed on each vessel. Samples that remained patent were injected with 50% (wt/vol) barium sulfate (Electron Microscopy Sciences) solution for improved lumen contrast. The scanning process was carried out with Inspect-X software (Nikon) and volumes were reconstructed with CT-Pro (Nikon). MicroCT data was analyzed in VGStudioMAX (Volume Graphics GmbH, Heidelberg, Germany). The three-dimensional scan data was analyzed first for stent fractures and overall structural integrity. Samples still containing calcium deposits were then analyzed for calcium content by adjusting the display window to show mineralized areas. When possible, areas of high restenosis were visualized by highlighting the vessel tissue or by injecting a barium sulfate contrast agent. Soft tissue contrast was minimal due to the energy levels being above 100kV and the presence of beam hardening artifact from the metal stents. Traditional two dimensional x-ray micrographs were taken using the same equipment in both *en face* and lateral orientations.

Histology

Samples were dehydrated through graded alcohols and then infiltrated in Technovit 7200 (Heraeus Kulzer, Wehrheim, Germany) methacrylate resin according to the manufacturer's instructions. Specimens were polymerized overnight in Technovit 7200 in the Exakt Light Polymerization Unit (Exakt, Norderstedt, Germany).

The Exakt System (Exakt, Norderstedt, Germany) microgrinder and high-precision diamond band saw were used for sectioning tissue samples(45). Three-dimensional reference points taken from MicroCT slice data and measurements taken from high resolution radiographs were used to cut a parallel face into the excess plastic mass

surrounding the specimen that aligned with the desired section. This end of the block was then affixed to a plastic mounting jig using Technovit 4000 adhesive (Heraeus Kulzer, Wehrheim, Germany). Next the diamond saw was used to split the block through the targeted area of interest, creating two opposing block faces within the desired region. The piece of the plastic block that was not attached to the jig was mounted on its own plastic mounting jig and faced in the same manner. This technique provides two block faces in the area of interest, on which a final polished thin plastic slide could be attached with cyanoacrylate glue (Technovit 7210, Heraeus Kulzer, Wehrheim, Germany). The final thin plastic slide was then cut from the block using the diamond saw 300 microns away from the slide. The resulting thin section was ground to a target thickness of 50 microns using progressively finer sandpaper on the microgrinder and then polished using silicon dioxide 4000 grit paper and stained.

Slides are stained as follows: (1) Etch slides for 2 minutes in 2% formic acid solution (vol/vol) (2) 5 minutes in 50% EtOH (vol/vol) (3) On a hot plate set to 55^{o} C, place a bead of Gill's #3 Hematoxylin (Electron Microscopy Sciences) over the specimen and allow to stain for 35 minutes (4) Rinse in distilled water and stain in a 50%/50% mixture of Eosin Y (Electron Microscopy Sciences) and Phyloxine B (Electron Microscopy Sciences) (vol/vol) (5) Rinse in distilled water and clear in 50% EtOH (vol/vol) with 2-3 drops of Acetic Acid (Electron Microscopy Sciences). The slides should be left uncoverslipped and examined microscopically under a small amount of immersion oil.

Digital Slide Imaging

All digital slide images were taken using an Aperio digital slide scanner (Aperio, Vista, CA, USA). This scanner is capable of images at 83x resolution that can be viewed at any magnification. Furthermore, built-in analysis and measurement tools enable easy quantification and description of results.

4. RESULTS

Case 1: Ruptured Soft Plaque

This case involves an acute implant in a 68 year-old female in the proximal right coronary artery. According to records, the patient presented with acute myocardial infarction with 100% stenosis of the RCA. Following stenting there was no measured reflow in the RCA. The patient died moments after catheterization. Present in the RCA was a stent identified by CT scanning as a Boston Scientific Taxus paclitaxel eluting stent. Analysis of the stent by X-ray and CT shows crushing and distortion of the stent body and damage to the ends of the stent: this finding is most likely iatrogenic (Figure 1A). Due to the collapsed nature of the vessel no contrast material was injected into the lumen. The vessel was decalcified prior to accessioning.

To evaluate the aftermath of this clinical intervention serial sections were taken of the entire vessel to attempt to locate the culprit lesion. A total of 10 sections were produced and examined microscopically for signs of rupture, thrombus formation, or hemorrhage.

Histology sections in the proximal and distal regions show multiple concentric complicated to fibrolipid plaques forming layered “piggyback” lesions that, prior to stenting, produced an approximately 50% lumen stenosis involving 90% of the circumference of the internal elastic lamina. Contralateral to the largest vulnerable plaque is a smaller, mildly calcified fibrolipid plaque with a thicker fibrous cap and a smaller lipid core. All lipid plaques in the wall of the vessel show hemosiderin-laden macrophages and erythrocytosis, indicative of older plaques. Post-stenting, the vessel lumen within the stent is nearly 100% patent. The site of rupture of the vulnerable plaque was located contralateral to the calcified lesion in the middle portion of the stent (Figure 1B). Deployment of the stent struts were not circumferential and were unevenly distributed. Several struts were embedded in the ruptured athermanous material penetrating into the lumen (Figure 1B, Green Arrows). The loose nature of the

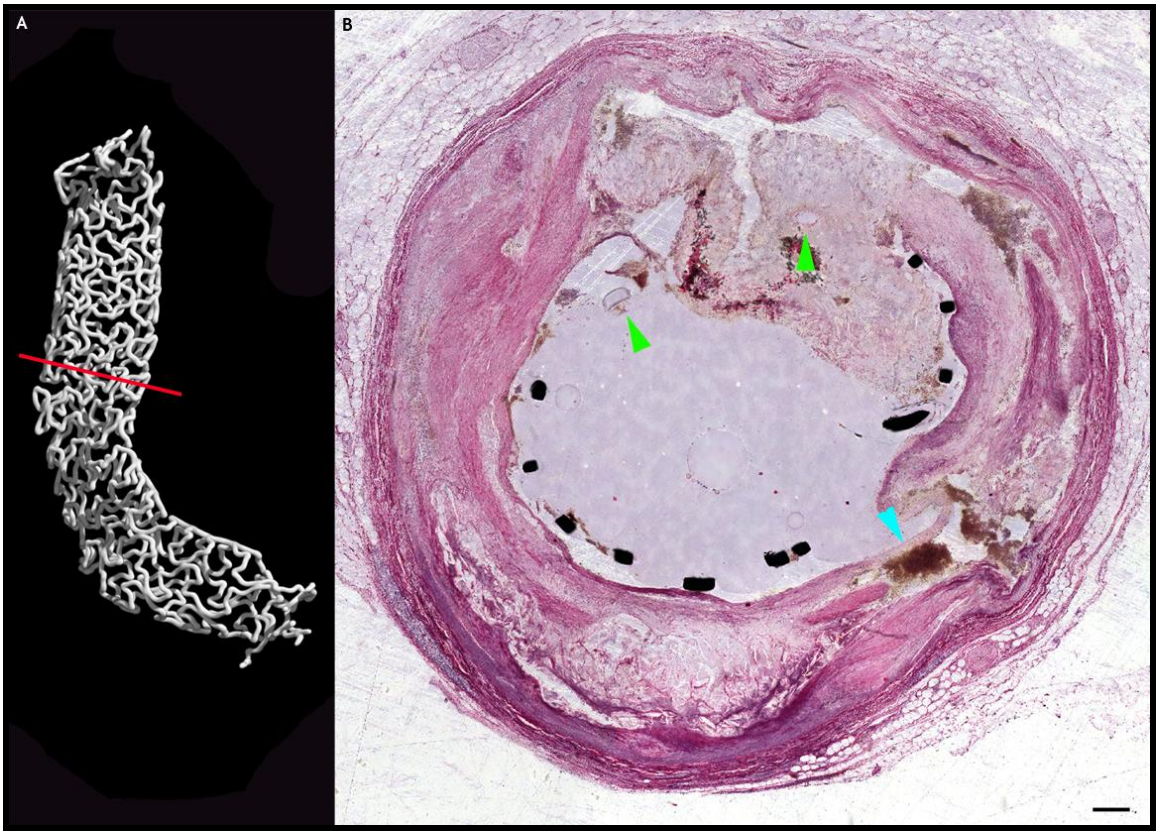

Figure 1: Vulnerable Plaque Rupture. Green arrows indicate the ruptured soft plaque core; blue arrows indicate evidence of acute hemorrhage into the plaque. 300 micron scale bar.

surrounding material led to the struts being lost during the cutting process, but the void where they were is still visible. Signs of acute hemorrhage were observed in this region as well, with evidence of acute bleeding between the media and adventitia layers in this and other sections distal to the rupture site (Figure 1B, Blue arrow). A nidus of ruptured plaque material can be seen occupying roughly 20% of the lumen, this material is not covered with endothelium. There are acute granulomatous infiltrates of neutrophils and some macrophages present in the ruptured material and in the vessel wall near the site of rupture. Downstream of the rupture site accumulations of platelets, enmeshed erythrocytes, and fibrin are observed along the vessel wall adhered to struts in the lumen and occupying the lumen itself. Stent struts observed microscopically show no signs of

endothelialization, consistent with an acute implantation. There were no signs of medial disruption.

Case 2: Acute Dissection

This case is an acute implant in a 60 year-old male in the proximal left main artery. According to records, the patient presented with acute coronary syndrome with 100% stenosis of multiple arteries in the left main and its branches. Following stenting there was a reported 10% stenosis, however runoff was still poor. Regardless of stenting the patient had already developed significant myocardial infarction that led to his death.

Present in the proximal left main was a stent identified by CT scanning as a Medtronic Integrity bare metal stent. Analysis of the stent by X-ray and CT shows crushing and distortion of the stent body and with multiple fractures and incomplete deployment hindered by the presence of a severely calcified vessel wall (Figure 2A). Furthermore, CT imaging shows the proximal end of the device deployed over a branch artery that is also heavily calcified. Of note, a broken strut can be seen protruding into the wall of the vessel between two calcified lesions on the proximal end of the vessel (Figure 2A, green arrows). Due to the collapsed nature of the vessel injection of contrast material into the lumen was unsuccessful. Remnants of the contrast material are rendered as gray in the microCT reconstruction, and fragments can be seen in the lumen of the vessel on histology (Figure 2). The vessel was not decalcified prior to accessioning; calcium is rendered as blue in the image.

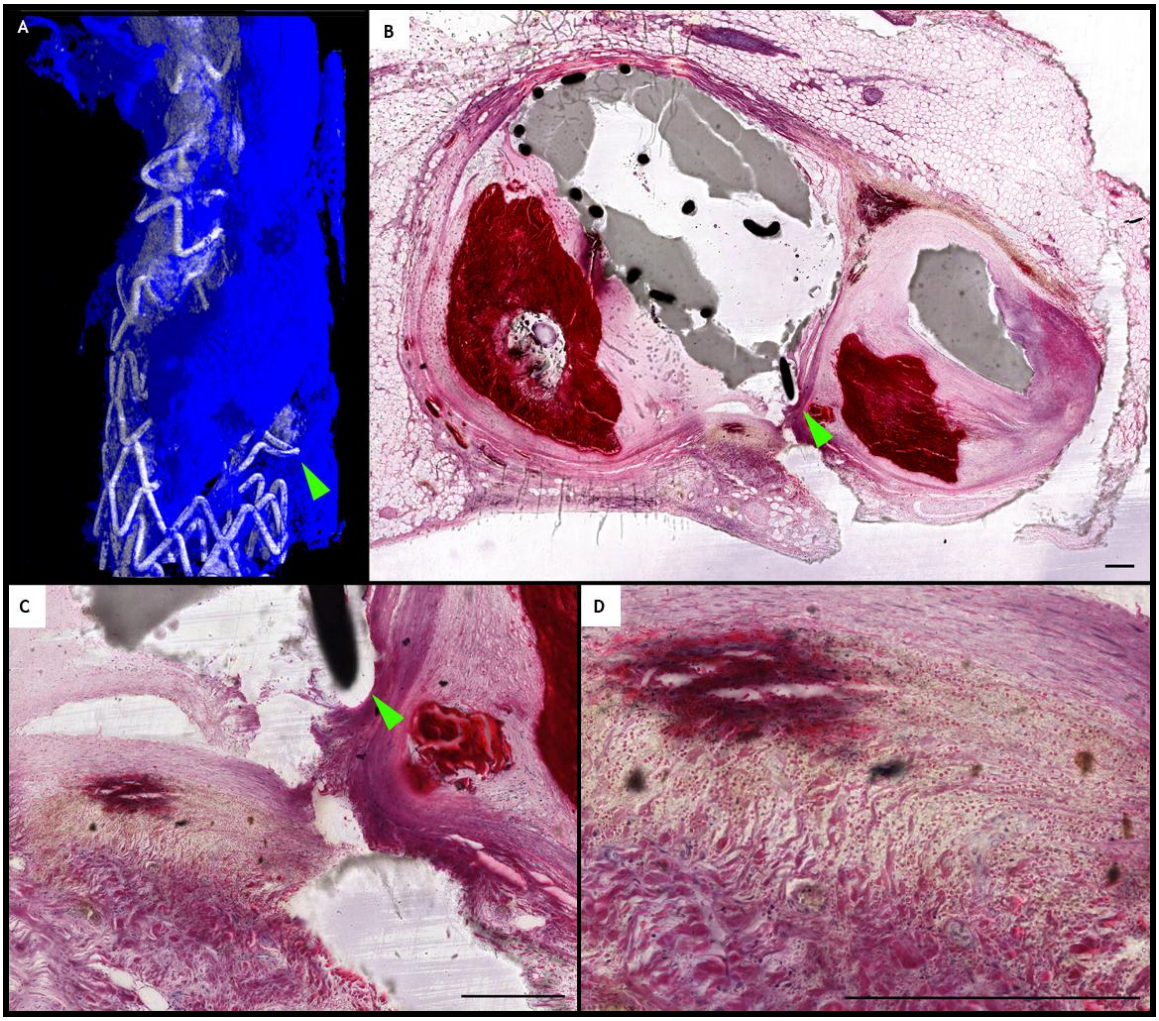

Figure 2: Calcified Plaque Dissection. (A) the strut protruding into the vessel wall (green arrow), mineralized plaque is shown in blue. (B) Shows the dissection site and protruding strut (green arrow). (C) shows a magnified view of the dissection site. (D) Shows the edematous hemorrhage with extravagation of erythrocytes. 300 micron scale bars.

In such a heavily calcified lesion the most probable location for stent deployment complications would be regions where the soft tissue could be damaged in between the calcified plaques. Targeted histology sections were directed toward a broken strut protruding into the lumen, as well as several millimeters proximal and distal to the site. A total of 10 sections were produced proximal and distal to the protrusion site and examined microscopically for signs of rupture, thrombus formation, or hemorrhage.

Histology sections at the rupture site show a multiple, concentric complicated plaques with severe multifocal to confluent areas of mineralization that, prior to stenting, produced an approximately 60% lumen stenosis involving 60% of the circumference of the internal elastic lamina. Similar calcified plaques can be seen in the branch arteries immediately adjacent to the stented artery. MicroCT confirms that the mineralized plaque is continuous with the mineralized plaque in the proximal left main. Contralateral to the mineralized plaque, the media of the vessel wall is very thin with the struts of the stent deforming the media and coming very close to the adventitial collagen. Several struts on the contralateral side were away from the vessel wall in the lumen, most likely due to handling artifact. The protruding stent can be seen dissecting the vessel wall through the media (Figure 2C green arrow). Surrounding the dissection site are signs of acute hemorrhage and edematous bleeding between the media and adventitia (Figure 2D). There are signs of mild acute granulomatous infiltrates of neutrophils and some macrophages present in the hemorrhaged material and in the vessel wall near the site of rupture. Sections taken proximal and distal to the rupture site confirm the length of the dissection to be several millimeters long, corresponding to the small gap between the mineralized plaques of the proximal left main and its branch artery; both of which show signs of deflection and separation on microCT. Stent struts observed microscopically show no signs of endothelialization, consistent with an acute implantation. There was no evidence of thrombus formation either local or remote.

Case 3: Vulnerable Plaque Erosion and Thrombosis

This case involves an acute implant in a 62 year-old male in the proximal left circumflex coronary artery. According to records, the patient had a stent implanted 1 week prior to admission for acute myocardial infarction. At autopsy there were multiple healed, acute, and sub-acute infarcts found in the heart muscle downstream of the implant site. It should be noted that the patient did not take Plavix due to cost issues.

Present in the proximal left circumflex obtuse artery was a stent identified by CT scanning as a Boston Scientific Liberte drug eluting stent. Analysis of the stent by X-ray and CT show an intact device with moderate distortion of the proximal region, most likely due to handling and extraction artifact (Figure 3A). The vessel contained many focal to confluent mineralized plaques around the middle region of the stent, shown in dark gray. Because of the presence of post-mortem clotted blood the lumen could not be injected with contrast material. The vessel was not decalcified prior to accessioning.

Targeted histology sections were taken from the most proximal region of the stent just before the damaged region. (Figure 3A, red line). Additional sections were taken several millimeters distal to the targeted site. A total of 9 sections were produced and examined microscopically for signs of rupture, thrombus formation, or hemorrhage.

Histology sections at the target site show a large, concentric soft atheromatous plaque with a lipid and cholesterol core and two large areas of focal to confluent mineralization located on opposite sides of the vessel that, prior to stenting, produced an approximately 85% lumen stenosis involving 100% of the circumference of the internal elastic lamina. The lumen of the vessel at this level is dominated by a “chicken fat and currant jelly” post-mortem blood clot that continues downstream to the distal end of the vessel (Figure 3B). The athermanous plaque shows signs of erosion and minimal endothelial coverage at the aneurismal extension of the plaque into the lumen (Figure 3 B-C, green arrows). Peristrut fibrin deposition is present around all of the stent struts, along with apparent lack of endothelialization between or upon the stent struts.

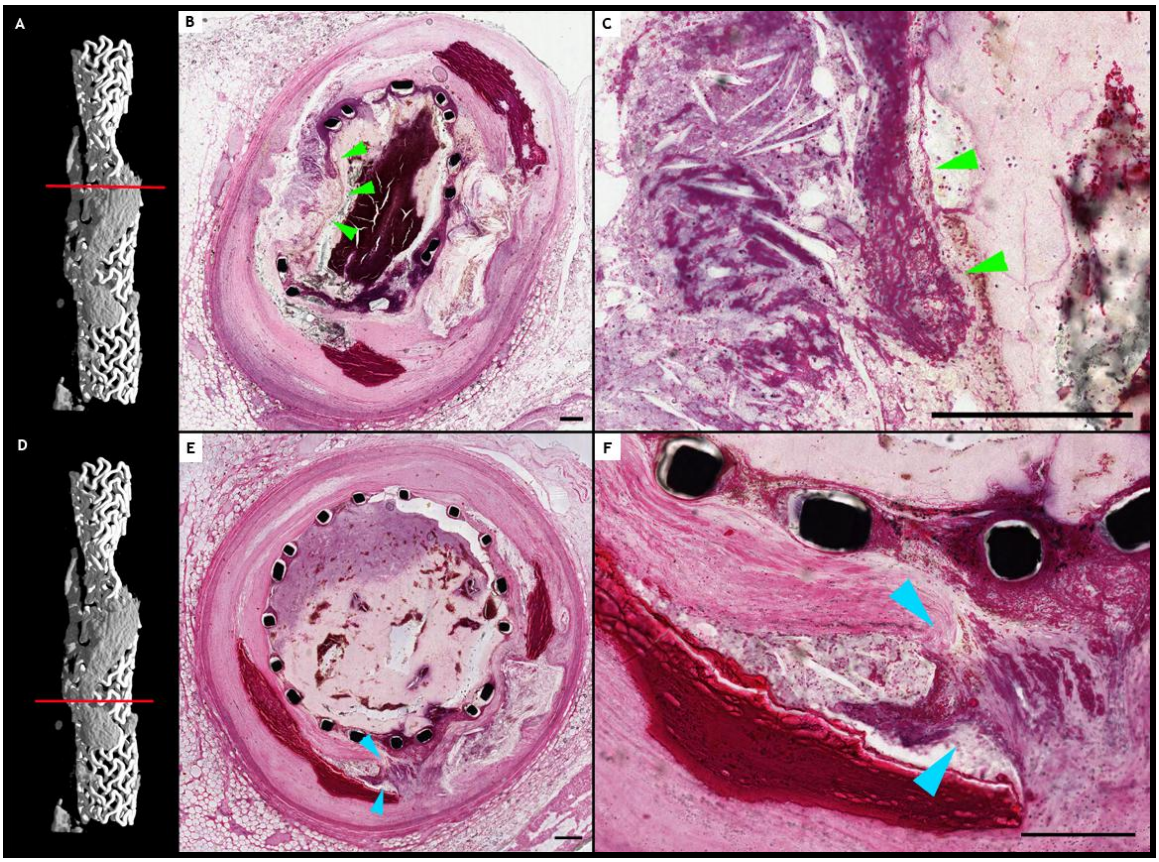

Figure 3: Effects of No Antiplatelet Therapy. (A, B, C) show the site of erosion of the soft plaque, 300 micron scale bar. (D, E, F) show the location of focal rupture with infiltration of erythrocytes and fibrin into the center of the plaque, 300 micron scale bar.

There are signs of mild to moderate granulomatous infiltrate present in the plaque as well as the fibrous accumulations along the vessel wall. Sections taken distal to the target site show extensions of the fibrous accumulations along the vessel wall and around the stent struts (Figure 3 D-F, blue arrows). Erythrocytes in the core of the plaque, with extensive fibrin accumulation can be seen in sections of the middle portion of the stent with fibrin lipid material exposed to the lumen (Figure 3 D-F, blue arrows). Port mortem blood clotting also obscures the vessel lumen in the proximal sections. There appears to be strong evidence of the formation of a thrombogenic nidus secondary to plaque rupture proximal to section shown in figure 3; however, because of handling damage sections could not be taken of this area.

Case 4: Mural Thrombus

This case is an acute implant in a 63 year-old male in the proximal left circumflex obtuse artery. According to records, the patient presented with acute coronary syndrome prior to stenting. Following stenting there was a reported <10% stenosis, however the patient died moments later of a peri-procedural acute myocardial infarction.

Present in the proximal left circumflex obtuse artery was a stent identified by microCT scanning as a Cordis (Johnson and Johnson) sirolimus eluting stent. Analysis of the stent by X-ray and CT shows an intact device with no evidence of disruption or fracture (Figure 4A). The stent was slightly bent in the region of the third-most proximal ring, an area that also contains a small, mineralized plaque. In addition microCT imaging shows the proximal end of the device deployed over a branch artery. The lumen was injected with contrast material, shown in gray on the reconstruction. The vessel was not decalcified prior to accessioning; calcium is rendered as dark gray in the image.

Targeted histology sections were taken from the bent region of the stent near the calcified plaque (Figure 4A, red line). Additional sections were taken several millimeters proximal and distal to the targeted site. A total of 3 sections were produced and examined microscopically for signs of rupture, thrombus formation, or hemorrhage.

Histology sections at the target site show a large, concentric fibrous plaque with a lipid and cholesterol core and small multifocal to confluent areas of mineralization that, prior to stenting, produced an approximately 70% lumen stenosis involving 100% of the circumference of the internal elastic lamina. Sections proximal to the target site show an old, dense, organized mural thrombus with a fibrous cap roughly 100 micrometers thick on the luminal side. This feature continues along the length of the stented vessel and can be seen in the target and distal sections as well.

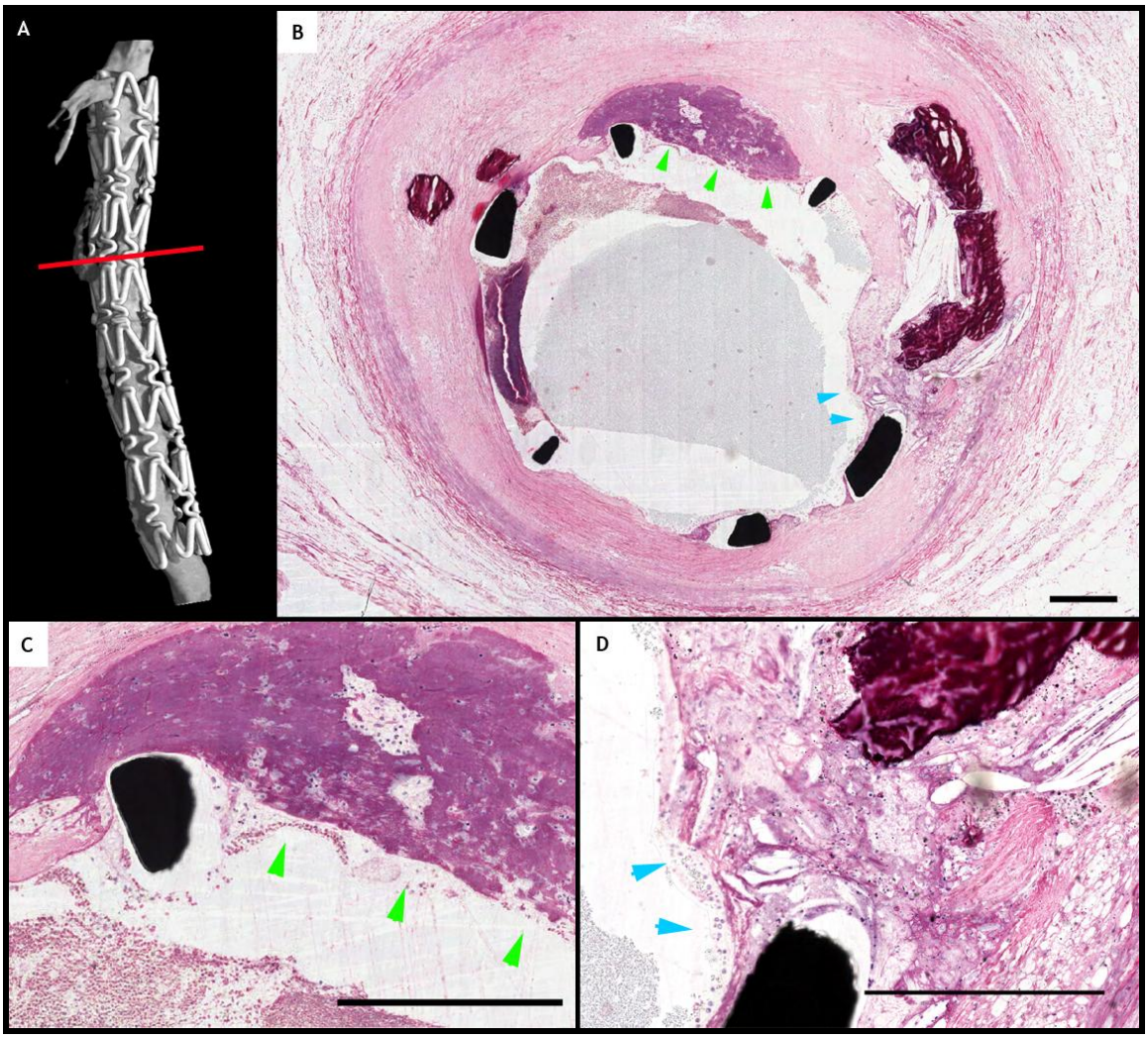

Figure 4: Mural Thrombus Dissection. (A) Red line representing the plane of sectioning distal to a branch artery near a bend in the stent. (B) Showing the mural thrombus (green arrows) with dissected fibrous cap and plaque rupture site (blue arrows). (C) Showing a closer view of the exposed mural thrombus (green arrows). (D) Showing a closer view of the ruptured plaque (blue arrows) adjacent to focal mineralization. 300 micron scale bars.

In the target section, however, the fibrous cap is pulled away from the wall and the thrombus is exposed to the lumen (Figure 4B, 4C green arrows). Just lateral to the mural thrombus is the mineralized lipid and cholesterol core of the fibrous plaque. On one end of the plaque a stent strut can be seen intruding into the core of the plaque, exposing the lipid and collagen substrate to the lumen of the vessel (Figure 4D, 4B blue arrows).

There are signs of mild acute granulomatous infiltrates of neutrophils present in the vessel wall near the site of rupture. Sections taken distal to the rupture site show similar infiltrates, as well as platelet and fibrin accumulation around the stent struts and along the vessel wall. MicroCT confirms the formation of in-stent fibrous accumulations distal to the target section with a gradual tapering of the luminal area starting just distal to the bend in the stent. Stent struts observed microscopically show no signs of endothelialization, consistent with an acute implantation; however, many of the struts are covered with accumulations of fibrin and enmeshed erythrocytes. There appears to be strong evidence of the formation of a thrombogenic nidus at the target section location that may have been sending emboli downstream, consistent with clinical observations.

Case 5: Overexpansion Contralateral to a Hard Plaque

In this case a 76 year-old female presented with acute coronary syndrome and died after coronary artery bypass grafting (CABG). Present in the right coronary artery were BMS. The most proximal was collected, decalcified, and stored in archive at the Texas Heart Institute (THI) before submission to our lab for processing. This stent, according to record, was implanted 2 years prior to the demise of the patient. Analysis of the stent by X-ray and CT *in situ* revealed a focal over-expansion of the stent struts (Figure 5, green arrows) contralateral to a series of struts that remained under-deployed.

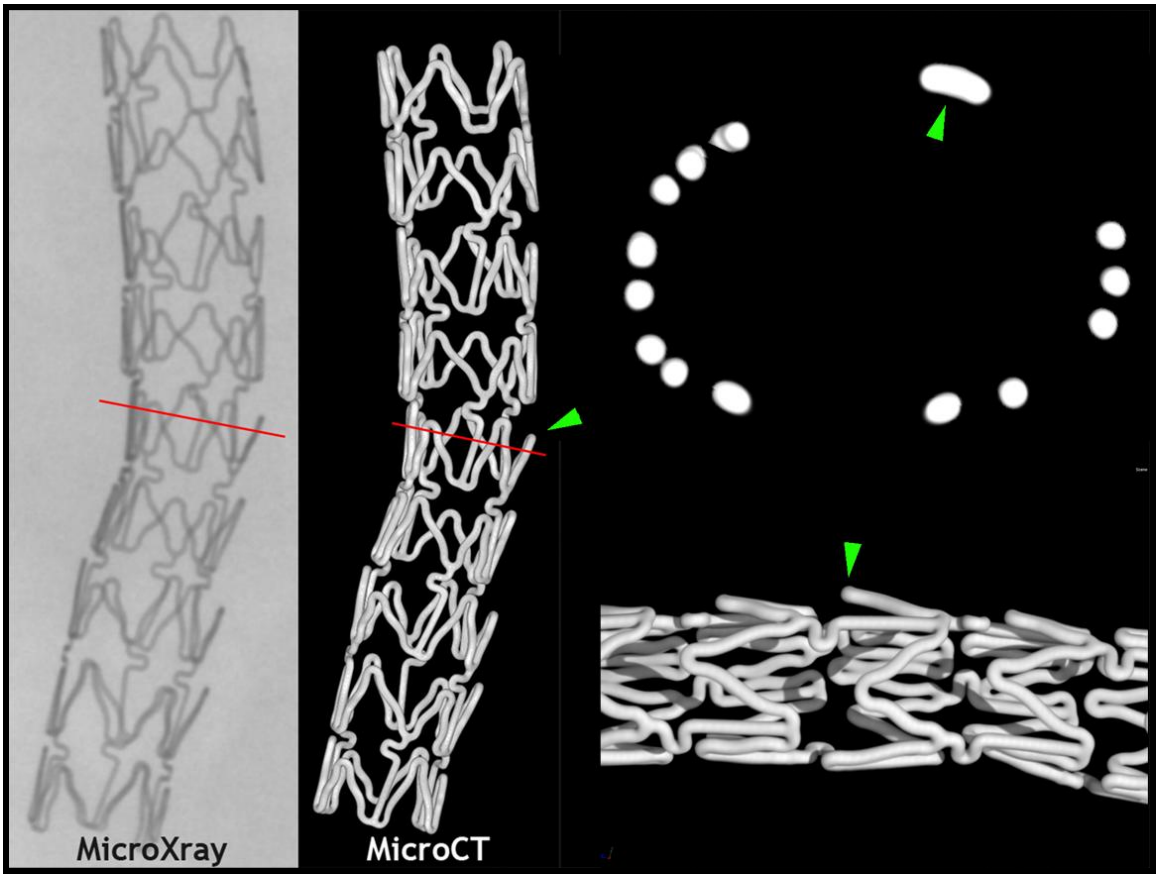

Figure 5: Over-Expanded Strut Contralateral to a Calcified Plaque. X-ray micrograph and MicroCT reconstructions of the implant. Green arrows indicate the over-expanded strut. Red line indicates the target section for histology. MicroCT cross section is at the level of the red line.

Unfortunately, this vessel was decalcified prior to receipt at our lab; therefore the extent of the presumed calcification in the region of the deformation could not be characterized by radiological imaging alone. To observe the vessel morphology at the site of the deformed strut, a section was taken that intersects where the strut protrudes into the vessel wall and the presumed calcific lesion on the opposite side (Figure 5, red line). When this cross section is isolated in the CT volume the uneven distribution of struts suggests possible incomplete expansion at the time of implantation (Figure 5).

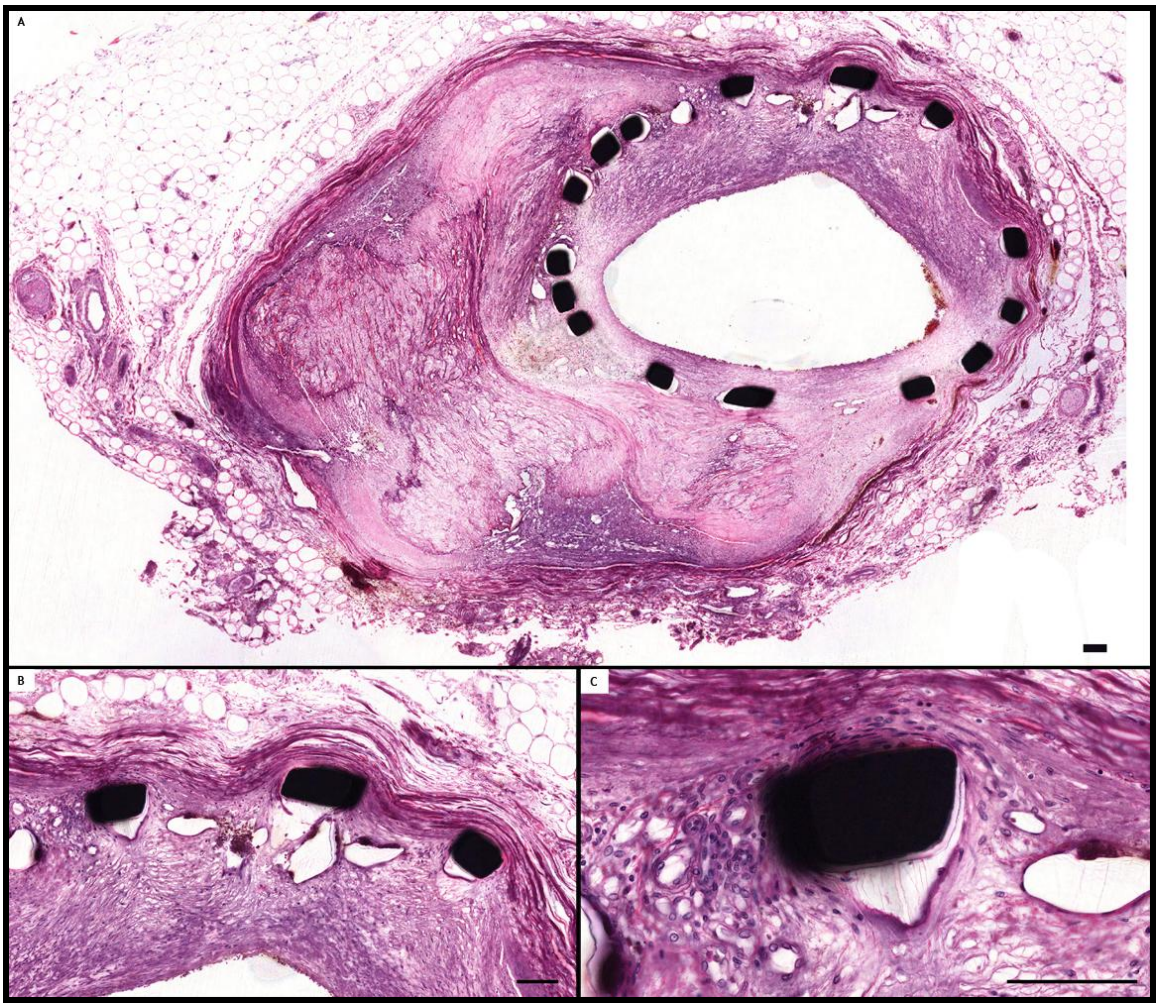

Figure 6: Internal Elastic Lamina Rupture Site. (A) Subgross view of the entire section. (B) Site of medial disruption by over-expansion. (C) Close-up view of the peristrut region at the rupture site. 300 micron scale bars.

Histology sections of this area show an eccentric plaque that, prior to stenting, produced an approximately 50% lumen stenosis involving 25% of the circumference of the internal elastic lamina (Figure 6). This is primarily a fibrolipid plaque with areas of focal to confluent mineralization at the center of the substrate. This plaque formed a dense, unyielding, barrier to the expansion of the struts of the stent within its proximity that resisted the expansion force of the angioplasty balloon. The force was redirected towards the path of least resistance (toward the contralateral side) and led to the overexpansion of

the struts in that area. Microscopic evidence supports this theory due to the observed uneven distribution of the stent struts opposite the plaque, and the presence of stent struts outside the internal elastic lamina that are resting in the media of the vessel (Figure 6b). Upon closer inspection of a different region of the stented lesion, distal to the first section in the second-most distal ring of struts, we found a fragment of the internal elastic lamina resting within the media of the vessel (Figure 7A, green arrow).

To confirm the extent of the internal elastic lamina rupture, serial sections were taken along the length of the stented lesion. All sections contained dissected portions of the internal elastic lamina and suggested that the observed damage is a longitudinal tear of the internal elastic lamina along the length of most of the stent. This acute damage invoked a healing and immune response to both the disruption of the elastic lamina and the presence of the foreign body. The effects of which can be seen most easily by the in-stent restenosis present along the length of the vessel that occupies, on average, 40% of the lumen area (Figures 6,7). The cellular composition of the areas of restenosis, however, is reminiscent of a healthy injury response. The endothelial cell layer is smooth and continuous, and there is no evidence of thrombus or thrombogenic areas in contact with the lumen. The substrate surrounding the stent struts and within the smooth muscle tissue contains a neovascular blood supply that is largely clear of debris, and only a few struts showed evidence of peristrut associated material (Figure 6B, 6B, green arrows).

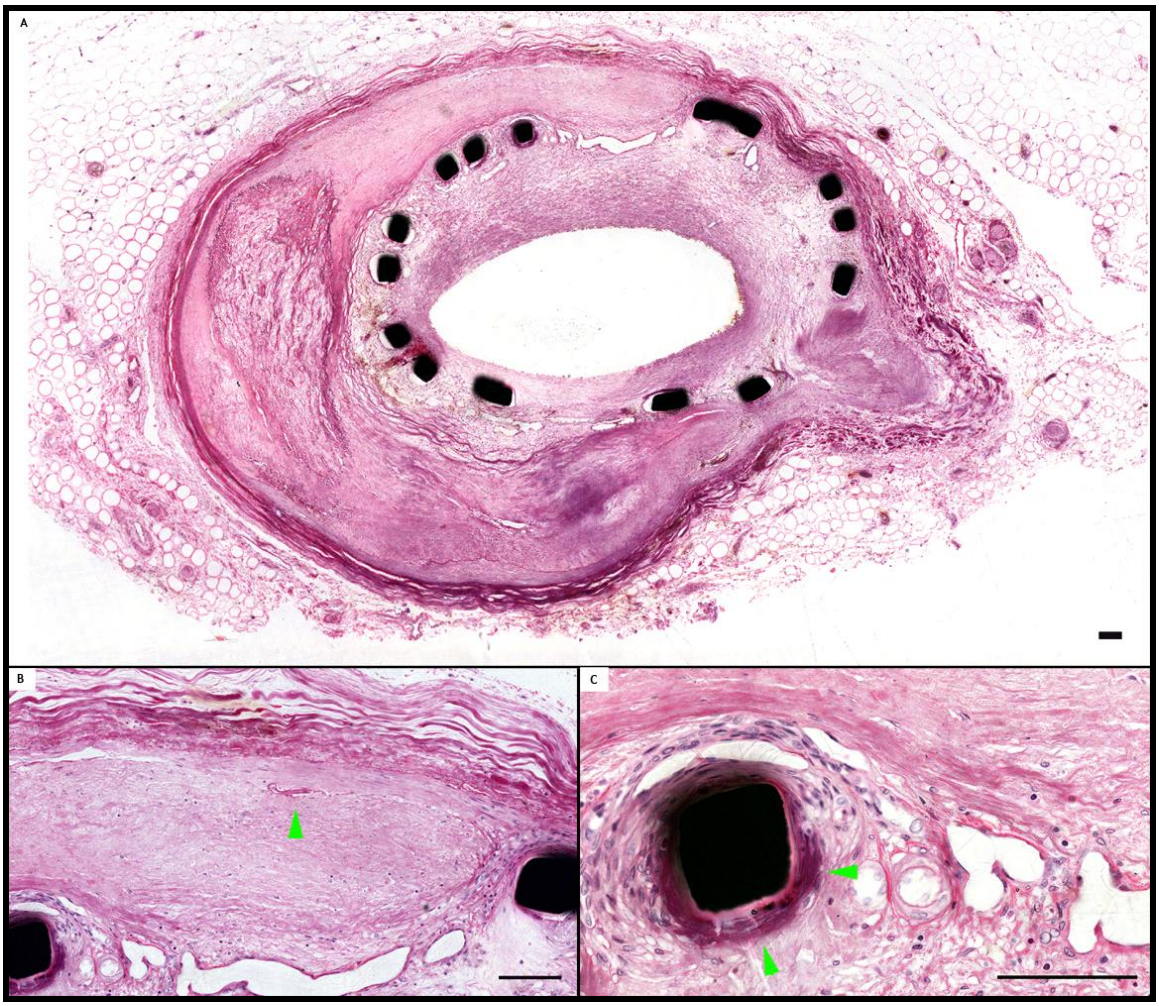

Figure 7: Distal Rupture Site. (A) Subgross view of the entire section. (B) Ruptured internal elastic lamina (green arrow). (C) Peristrut amorphous material caused by trapping of erythrocytes and fibrin by neointimal proliferation (green arrows). 300 micron scale bars.

Some regions of the vessel had minor areas of enmeshed erythrocytes and fibrin, however there was no evidence of a lasting inflammatory response. The duration of this implant was 2 years, so the scarcity of multinucleated giant cells, neutrophils, and lymphocytes is expected given the time since the original insult. Restenosis occupying 40% of the lumen of a blood vessel would not have generated clinical signs in the patient.

Case 6: Long-Term Drug Eluting Stent

This chronic case involves a long-term drug eluding implant in a male of unknown age for duration of 6 years prior to receiving a heart transplant in August 2010. Present in the left circumflex coronary artery (LCX) was a stent identified by CT scanning as a Johnson and Johnson Cordis sirolimus eluting stent. Analysis of the stent by X-ray and CT revealed fragmentation of the stent at a branch artery near the proximal end of the vessel and in the middle of the main body of the stent (Figure 8, green arrows). Contrast material injected into the lumen revealed no major disruptions or plaques along the length of the vessel.

Each ring of struts was sectioned to observe the host tissue response to the drug infused polymer coating. A total of 9 sections were produced, 2 of which intersected with the fragmented portions of the stent, and examined microscopically for signs of delayed healing, endothelial disruption, or medial rupture

Histology sections in the proximal area show an eccentric fibrolipid atherosclerotic plaque with cholesterol clefts and a lipid core that, prior to stenting, produced an approximately 60% lumen stenosis involving 40% of the circumference of the internal elastic lamina (Figure 9). Post-stenting, the vessel lumen within the stent is nearly 100% patent with minimal in-stent restenosis. Contralateral to the plaque in this section, and in the other sections, is evidence of rupture of the internal elastic lamina due to the expansion of the stent, along with medial disruption and degeneration.

The media on the contralateral side is almost completely degenerated leaving only a small amount of space between the implant and the adventitia (Figure 9b). In the distal portion of the stent, just distal to the strut fracture, the fibrolipid plaque becomes more calcified, but still retains its prominently visible lipid and cholesterol core.

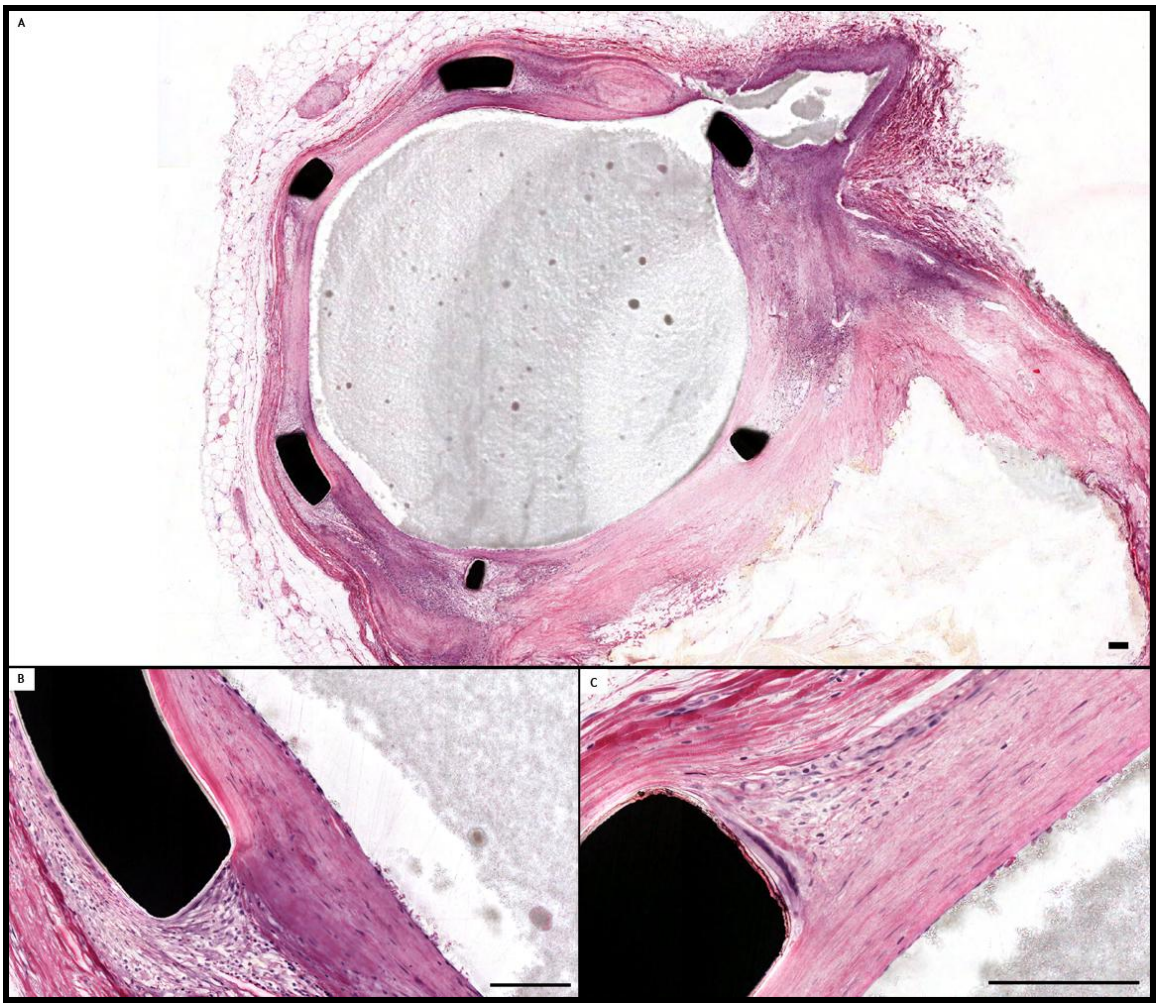

Figure 8: Proximal Drug-Eluting Stent. The proximal region of the DES is deployed over a branch artery. At this level the struts show complete coverage, except for the strut over the lumen of the branch artery. (B, C) show a completely covered strut with dense fibrous cap. 300 micron scale bar.

Contralateral to the plaque there is still evidence of medial disruption; however at this level there is an immature early resolving thrombus with mixomatous material covering two of the stent struts (Figure 9). Accompanying this thrombus is a moderate to severe cellular response over two of the struts, and a limited cellular reaction over the other four struts adjacent to the plaque. The nidus of the thrombus was located approximately 2.5mm proximal to this section and seems to be involved with a portion of disrupted endothelium near the fractured strut.

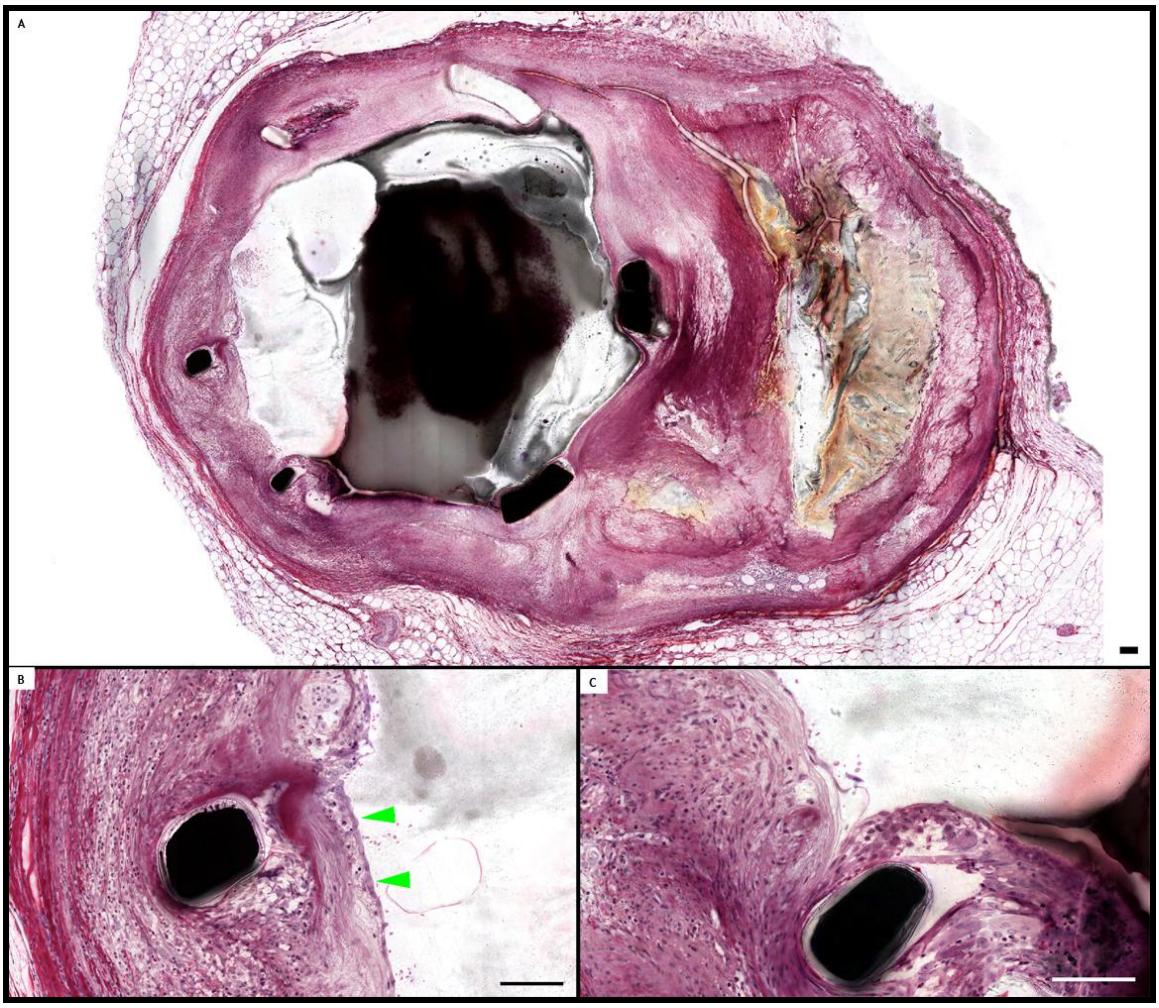

Figure 9: Distal Drug Eluting Stent. The distal region of the DES show several unhealed struts still in contact with the vessel lumen. (B) shows the incomplete healing of the endothelium, and the poorly differentiated endothelial cells (green arrows). (C) shows a poorly covered strut surrounded by inflammatory cells and a loose matrix substrate. 300 micron scale bar.

Of the 72 struts observed microscopically roughly 40% (29 total), showed distinct multinucleated giant cell encasement. Out of the others, 17 had direct contact with the lumen, meaning they had little to no endothelial covering. Furthermore 40 struts showed a mild to severe cellular inflammatory response consisting of lymphocytes, macrophages, and scattered neutrophils indicative of the active healing. The health and maturity of the endothelium was also evaluated. Roughly 40% of the endothelium observed was poorly differentiated and had the appearance of large, puffy mesothelium

cells attempting to form a monolayer over the neointima and immature organizing thrombus noted on the distal portion of the vessel. The connective tissue substrate beneath the unhealed struts was a mixture of immature mixomatous and loose connective tissue.

Case 7: Complex Multiple Implantation

The last chronic case has a long and complicated history. The patient, a 62 year-old white male as of 2011, first had a PCI with stenting of the RCA in 2002. Seven years later the patient presented with an acute myocardial infarction (MI) and received 6 stents, a DES in the proximal and distal RCA, and 4 BMS in the middle RCA. The oldest implant was determined to be a Boston Scientific Liberte BMS. The Boston scientific Taxus DES shares a strut design with the Liberte DES, but was not FDA approved for use in the United States until 2003; therefore this implant must be the BMS variety. The BMS in the middle RCA implanted in November 2009 were determined to be Medtronic Crown stents. The DES implanted in the proximal and distal regions were identified as Boston Scientific Promus stents, approved by the FDA in 2008. The patient received a transplant in 2011. X-ray and CT analysis revealed diffuse to confluent calcific plaques along the length of the entire RCA (Figure 10B). The vessel was too long and articulated to reliably and safely inject contrast media into the lumen without risking complications with infiltration and embedding. The distal tip of the vessel needed to be cut 1 cm from the end in order to fit the entire vessel in the embedding mold, the cut portion was embedded alongside the main artery.

To approach such a long and complicated lesion, the vessel was divided into four portions (Figure 10A). In each section landmarks from the CT volume were noted. The first area of interest is a nodule of calcium between two sets of stent implants, both within the neointima of the older implant, and outside the struts of the newer implant (Figure 10F, Cut 4). A section was taken of the oldest of the stents in the middle-distal portion of the RCA (Figure 10H, Cut 6). A section was targeted towards the region of

the highest strut density, representing the overlap of five different stents at the same spot (Figure 10C, Cut 1). Further sections were also taken of each region evenly spaced along the length of the vessel. In total, 15 sections were obtained from the RCA.

Subgross evaluation of cut 1 (Figure 10C) shows the area of the RCA with the highest density of metal struts, totaling 5 stents in the same area. The oldest DES implant is shown pressing against the media of the vessel, which shows signs of degeneration (Figure 11A). Adjacent to one of the struts are trapped erythrocytes and fibrin (Figure 11A, green arrows). Within this DES are small nodules of focal calcification of the neointima (Figure 11B). Finally inside of these nodules, slightly depressing them as they rest against the neointima of the DES are 4 more BMS implanted in 2009. Although these implants are all greater than 2 years old, there is very little neointimal growth within the latest round of BMS implants, presumably due to the effects of the DES just underneath them. All but 2 struts are covered by endothelium; 2 struts are exposed to the lumen; and 2 struts shows fibrin accumulation with enmeshed erythrocytes (Figure 11A).

Moving distally roughly 1cm to cut 2 (Figure 11D) the DES is no longer present in the vessel wall. The calcified plaque is slightly larger and occupies 35% of the vessel wall and all 4 BMS implants can be seen. The oldest implant can be seen resting against the media, which is thinner here compared to the first section. The stent struts contralateral to the plaque were dislodged during handling and transport of the specimen. All but 3 struts are covered by endothelium. An athermanous plaque between the two oldest and two newest implants can be seen occupying roughly 30% of the neointima on that side. Within the plaque is a focal nodule of mineralization.

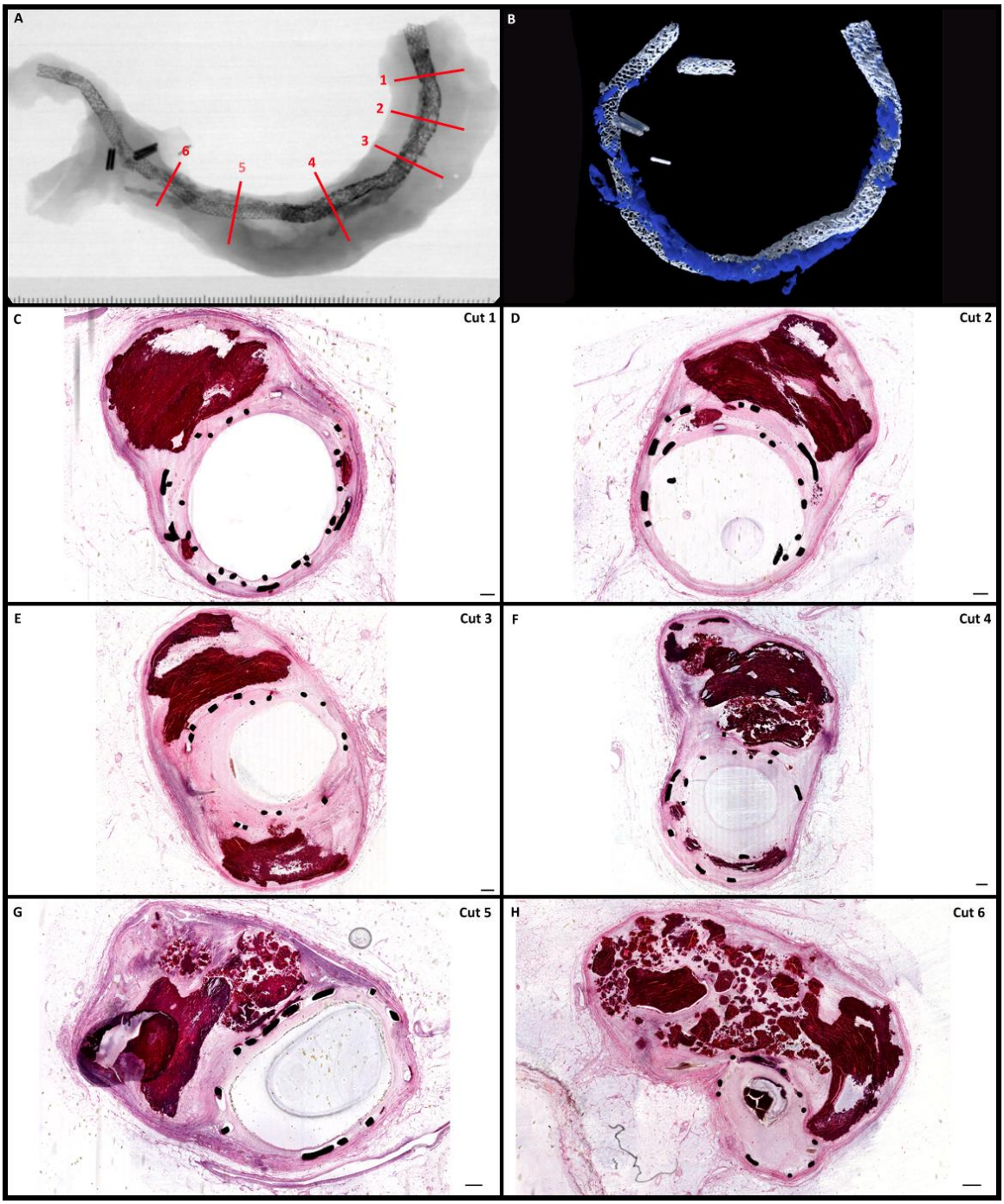

Figure 10: Subgross Sectioning Overview. X-ray and MicroCT renderings along with representative regions from the entire vessel are shown. 300 micron scale bar.

Approximately 1 cm distal to cut 2 is cut 3 (Figure 11E). Here the mineralized plaque becomes bilateral and occupies 80% of the media. Two BMS implants can be seen; one implanted 2 weeks before the other. The newer of the implants expanded the lumen of the older, and restored roughly 60% of flow through the vessel. A pair of over expanded struts can be seen pressing against the media on the right side of the slide. Adjacent to this area is a rupture of the internal elastic lamina, possibly due to bilateral constraint of the expanding balloon by the mineralized plaques, which led to a perpendicular overexpansion of the stent struts towards the un-mineralized side. Medial disruption also may have been the driving force behind the increased neointima proliferation seen in this area.

MicroCT analysis showed an area of pronounced mineralization within the stent struts of the older implant and the newer two implants placed two weeks earlier several centimeters distal to cut 3. The mineralized neointima plaque occupies roughly 45% of the circumference of the neointima and is measured on microCT to be several millimeters long. The primary mineralized plaque is larger still, occupying roughly 55% of the vessel wall contralateral to the neointima mineralization. The peri-strut substrate is a mixture of loose fibrin and mixomatous connective tissue and cells with a mild inflammatory infiltrate of neutrophils and macrophages, indicative of chronic irritation (Figure 11C). The presence of active inflammation and immature connective tissue is a marked change from the dense fibrous appearance of the peristrut regions seen in cuts 1-3. A clear rupture of the internal elastic lamina can be seen along the edge of the media (Figure 11D). Almost all of the outermost implant's struts can be seen in contact with, or infiltrating, the media. This information, combined with the internal elastic lamina rupture, possibly explains the marked increase in neo intima proliferation at this level; which produced a total in stent restenosis of roughly 60%.

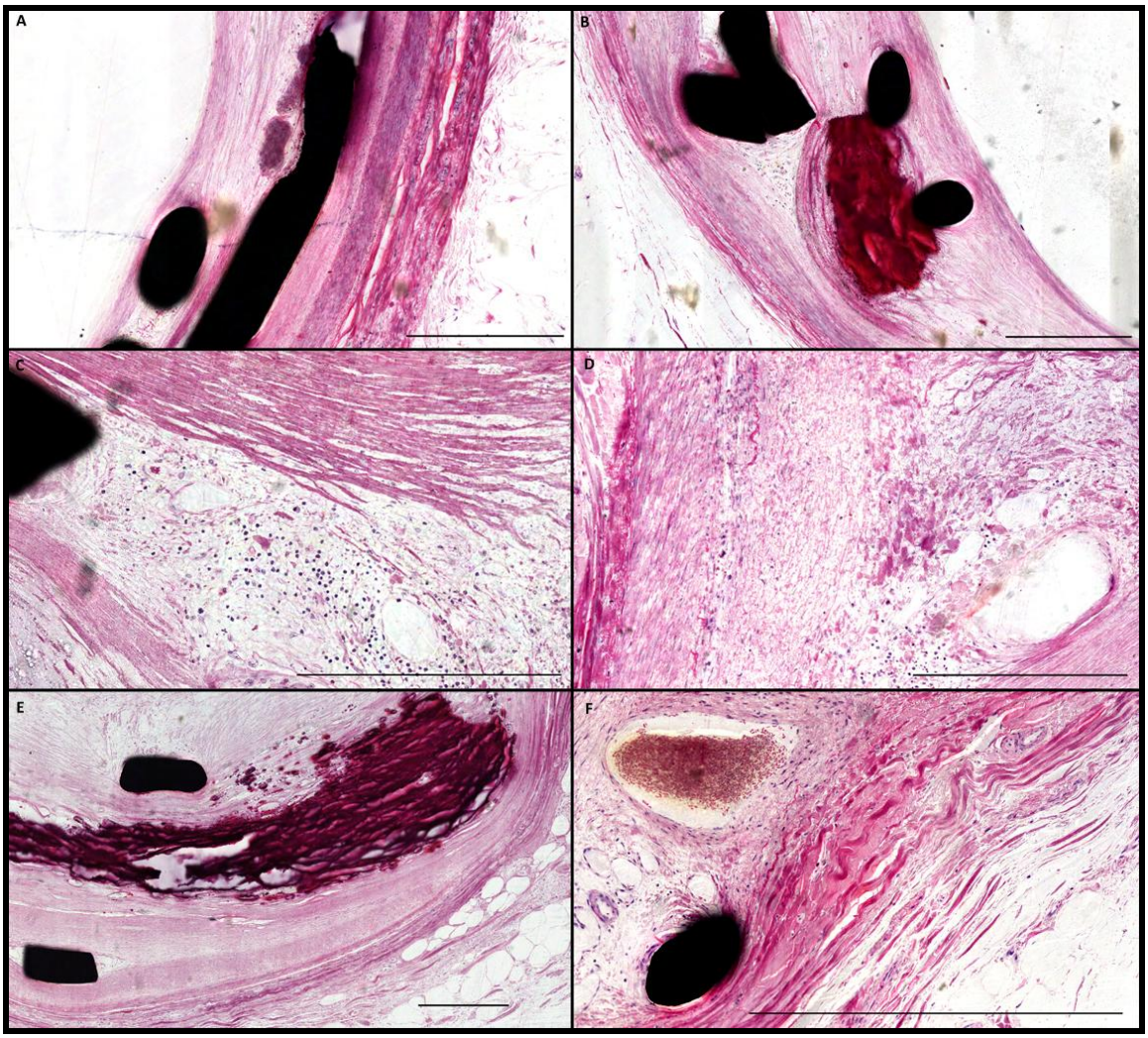

Figure 11: Specific Findings. High magnification of specific regions of the vessel show relevant findings. 300 micron scale bar.

The next section, cut 5 (Figure 10G, shows a mineralized plaque that is even larger; measuring roughly the same size as the stented vessel and occupying 55% of the vessel wall. The only stent in this area is one of the 2-year duration implants. Of note, the struts are in contact with the media of the vessel wall but do not penetrate the internal elastic lamina. There was no evidence of medial disruption, although the media is quite thin in this area similar to cuts 1 and 2. There is minimal neointima proliferation at this level, as the vessel lumen remains 95% patent.

The final section, Cut 6, represents the oldest of the implants. A bare metal stent implanted 9 years prior to transplant. The mineralized plaque is most pronounced at this level, dwarfing the size of the stented vessel and occupying 70% of the vessel wall. The plaque, prior to stenting, occupied over 95% of the vessel lumen. And when the BMS was implanted it expanded contralateral to the plaque and ruptured the internal elastic lamina, which cannot be seen on this slide due to degeneration of both the lamina and the media. Figure 11F shows the stent strut is resting on collagen in the adventitia, with no signs of a medial layer of smooth muscle or an internal or external elastic lamina. The neointima occupies 90% of the stented lumen, residual post explant blood can also be seen in the lumen.

5. DISCUSSION AND CONCLUSION

In the first acute case we located the definitive site where the vulnerable plaque ruptured, spilling its thrombogenic contents into the bloodstream. There was no way to tell if the rupture occurred before or after the stent was implanted, as rupture of a vulnerable plaque is sometimes the cause of acute myocardial infarction which would have led to the stenting of the artery. Demonstating the proof of concept of the ability to locate and observe the definitive site of a soft plaque rupture at autopsy reinforces the value of these techniques.

Case 2 involved the implantation of a series of stents in a heavily mineralized vessel. We believe the expansion force during implantation drove two large calcified lesions apart at a branch vessel, leading to a dissection of the wall of the vessel through the media and adventitia resulting in hemorrhage and edema of the surrounding tissue. Serial sectioning verified the extent of the dissection that traced back to the broken strut that was seen on microCT protruding into the wall of the vessel. Were it not for the cross-validation capabilities of histology and microCT we could not have been able to say for certain if the lesion was real or merely handling artifact.

Case 3 was originally an example of the deleterious effects of forgoing antiplatelet therapy after implantation of a DES. Further evaluation, however, revealed an acute vulnerable lipid plaque rupture that produced a thromboembolic nidus that sent emboli downstream to produce the small acute and sub-acute myocardial infarctions observed clinically. It is unfortunate that iatrogenic handling damage to the vessel obscured the definitive site of rupture, but evidence of the rupture such as erythrocytes and acute fibrin deposition within the plaque can be seen in serial section downstream from the supposed rupture site. Cases like these are a prime example of why clinical testing of interventional medical devices is so difficult; because the confounds of diseased arteries may obscure clinical outcomes based studies. However a direct pathology examination of the vessel revealed what was really going on.

Case 4 is another case where a ruptured soft plaque released its contents into the lumen of the vessel. An additional mural thrombus, however, adhered to the wall of the vessel that was covered with a fibrous cap. The cap can be seen on the proximal and distal most sections of the vessel where only the leading and trailing edge of the stent contacted the wall. However in the middle of the stent, when the stent expanded the lumen of the vessel, the thrombus was pressed through the struts and extruded into the lumen. The pieces of the thrombus that were dissected may have remained attached to the wall only to get lost during processing. Or rather, they may have also broken free to go downstream to contribute to the perioperative myocardial infarction that led to the patient's demise. This case is a good example of an off label use of a stent in the vicinity of a vulnerable mural thrombus. Evaluation of vessels like these at autopsy could generate information that will be relayed back to cardiologists to guide future off-label use of these devices.

In case 5 the cardiologists were wondering why the vessel was slowly continuing to become more stenosed two years after implant. Based on our observations the stent was over-expanded within the vessel producing a rupture of the internal elastic lamina contralateral to a calcified plaque. It was not necessarily an overabundance of expansion pressure at the time of implant. Rather the calcified plaque that occupied a large part of the vessel resisted the expansion of one side of the stent struts enough to direct the majority force of the expansion towards the opposite side. The presence of the metal device in the media of the vessel wall and the rupture of the internal elastic lamina led to a smoldering long term immune response that drove the expansion and proliferation of smooth muscle cells in the neointima.

In case 6 the DES, which should have completely eluted its entire drug load in the first few months of implant and allowed the healing process to finish was still suppressing the healing process around a majority of the stents 6 years after implant. Some of the struts showed signs of healing and encapsulation, but over the length of the stent a large number were still exposed to the lumen. In one region they were overlapping a branch

vessel and remained unendothelialized. Although there was a similar internal elastic lamina rupture and medial disruption found in this case when compared to case 5, the lumen was significantly more patent. Because the lumen remained patent this device would have been considered a success. No one would have known about the state of the stent struts in the lumen or the unhealed appearance of the peri-strut regions of this vessel had this evaluation not been done at the microscopic level.

In the last case, case 7, the complexity of the case presents many interesting implications for the evaluation of the healing response to these implants. Complex interactions such as; multiple BMS implanted in an old DES; the effects of medial disruption in the distal end of the vessel, and lack thereof in the proximal end on the healing process; and the rate of neointimal growth across multiple regions can be observed within the same specimen. The differences between disruption of the media and the subsequent healing response can be seen near both bare metal stents and drug eluting stents. Furthermore, atherosclerotic change to the neointima(4) over 9 years of implant duration, including mineralization and its response to repeat stenting can be seen; a phenomenon that has not been published before in the literature with this level of detail.

When processing the samples for histology, the microCT was invaluable for locating areas of interest and for validating the findings from histology. When questions arose about the three dimensional configuration of certain observations like the extent of the calcification in case 2, microCT data was able to provide the necessary information.

The quality of the histology sections that we produced is the real driving force behind the power of the observations. High resolution cellular detail gave us the ability to demonstrate the healing response in the chronic implants, as well as locate and isolate acute lesion sites. Using these techniques on a large scale as part of a routine autopsy of patients implanted with metal stents could provide a wealth of information for cardiologists and biomedical engineers and lead to tangible improvements in patient care.

REFERENCES

1. Roger VL, Go AS, Lloyd-Jones DM et al. Heart disease and stroke statistics--2012 update: a report from the American Heart Association. Circulation 2012;125:2-220.
2. Farb A, Boam AB. Stent thrombosis redux—the FDA perspective. N Engl J Med 2007;356:984-987.
3. Chan PS, Patel MR, Klein LW et al. Appropriateness of percutaneous coronary intervention. J Am Med Assoc 2011;306:53-61.
4. Buja LM. Vascular responses to percutaneous coronary intervention with bare-metal stents and drug-eluting stents: a perspective based on insights from pathological and clinical studies. J Am Coll Cardiol 2011;57:1323-6.
5. Farb A, Weber DK, Kolodgie FD, Burke AP, Virmani R. Morphological predictors of restenosis after coronary stenting in humans. Circulation 2002;105:2974-2980.
6. Marroquin OC, Selzer F, Mulukutla SR et al. A comparison of bare-metal and drug-eluting stents for off-label indications. N Engl J Med 2008;358:342-52.
7. Girod JP, Mulukutla SR, Marroquin OC. Off-label use of stents: bare-metal versus drug-eluting stents. Expert Review of Cardiovascular Therapy 2008;6:1095-106.
8. Oscar M, Faith S, Suresh M et al. A comparison of bare-metal and drug-eluting stents for off-label indications. N Engl J Med 2008;358:1-11.
9. Malik N, Gunn J, Holt C et al. Intravascular stents: a new technique for tissue processing for histology, immunohistochemistry, and transmission electron microscopy. Heart 1998;80:509-516.
10. Lubbe HBM, Klein CPAT, Groot K. A simple method for preparing thin (10 μm) histological sections of undecalcified plastic embedded bone with implants. Biotechnic & Histochemistry 2007;60:1-6.

11. Foerst J, Ball T, Kaplan A. Postmortem in situ micro-CT evaluation of coronary stent fracture. Catheter and Cardiovasc Interv 2010;76:527-531.
12. Jensen JK, Jensen LO, Terkelsen CJ et al. Incidence of definite stent thrombosis or in-stent restenosis after drug-eluting stent implantation for treatment of coronary in-stent restenosis. From western denmark heart registry. Catheter Cardiovasc Interv 2012:1-21.
13. Lüscher TF, Steffel J, Eberli FR et al. Drug-eluting stent and coronary thrombosis: biological mechanisms and clinical implications. Circulation 2007;115:1-9.
14. Mauri L, Hsieh W, Massaro JM, Ho KK, D'Agostino R, Cutlip DE. Stent thrombosis in randomized clinical trials of drug-eluting stents. N Engl J Med 2007;356:1020-1029.
15. Tsimikas S, Tsimikas S, Tsimikas S. Drug-eluting stents and late adverse clinical outcomes: lessons learned, lessons awaited. J Am Coll Cardiol 2006;47:1-6.
16. Wenaweser P, Daemen J, Zwahlen M et al. Incidence and Correlates of Drug-Eluting Stent Thrombosis in Routine Clinical Practice: 4-Year Results From a Large 2-Institutional Cohort Study. J Am Coll Cardiol 2008;52:1-9.
17. Iakovou I, Iakovou I, Schmidt T et al. Incidence, predictors, and outcome of thrombosis after successful implantation of drug-eluting stents. J Am Med Assoc 2005;293:2126-2130.
18. Nakazawa G, Finn A, John MC, Kolodgie FD, Virmani R. The significance of preclinical evaluation of sirolimus-, paclitaxel-, and zotarolimus-eluting stents. Am J Cardiol 2007;100:S36-S44.
19. Lyon R, Zarins CK, Lu CT, Yang CF, Glagov S. Vessel, plaque, and lumen morphology after transluminal balloon angioplasty. Quantitative study in distended human arteries. Arteriosclerosis, Thrombosis, and Vascular Biology 1987;7:306-314.

20. Schwartz RS, Huber KC, Murphy JG et al. Restenosis and the proportional neointimal response to coronary artery injury: results in a porcine model. J Am Coll Cardiol 1992;19:267-274.
21. Joner M, Finn A, Farb A et al. Pathology of drug-eluting stents in humans delayed healing and late thrombotic risk. J Am Coll Cardiol 2006;48:193-202.
22. Wilson GJ, Nakazawa G, Schwartz RS et al. Comparison of inflammatory response after implantation of sirolimus-and paclitaxel-eluting stents in porcine coronary arteries. Circulation 2009;120:141-149.
23. Farb A, Sangiorgi G, Carter AJ et al. Pathology of acute and chronic coronary stenting in humans. Circulation 1999;99:44-52.
24. Beusekom HM, Saia F, Zindler JD et al. Drug-eluting stents show delayed healing: paclitaxel more pronounced than sirolimus. European Heart Journal 2007;28:974-979.
25. Silva GV, Fernandez MR, Madonna R et al. Comparative healing response after sirolimus- and paclitaxel-eluting stent implantation in a pig model of restenosis. Catheter Cardiovasc Interv 2009;73:1-8.
26. Nakazawa G, Finn A, Joner M et al. Delayed arterial healing and increased late stent thrombosis at culprit sites after drug-eluting stent placement for acute myocardial infarction patients: an autopsy study. Circulation 2008;118:1138-1145.
27. Boer OJ, Wal AC, Becker AE. Atherosclerosis, inflammation, and infection. J Pathology 2000;190:237-243.
28. Chen YX, Ma X, Whitman S, O'Brien ER. Novel antiinflammatory vascular benefits of systemic and stent-based delivery of ethylisopropylamiloride. Circulation 2004;110:3721-3726.
29. Waksman R, Barbash IM, Dvir D et al. Safety and efficacy of the XIENCE V everolimus-eluting stent compared to first-generation drug-eluting stents in contemporary clinical practice. Am J Cardiol 2012;109:1-7.

30. Waksman R, Pakala R, Baffour R et al. Efficacy and safety of pimecrolimus-eluting stents in porcine coronary arteries. Cardiovascular Revascularization Medicine 2007;8:259-274.
31. Takayama T, Hiro T, Akabane M et al. Degree of neointimal coverage is not related to prevalence of in-stent thrombosis in drug-eluting stents: a coronary angioscopic study. International J Cardiol 2012;156:1-3.
32. Palmerini T, Biondi-Zoccai G, Riva D et al. Stent thrombosis with drug-eluting and bare-metal stents: evidence from a comprehensive network meta-analysis. Lancet 2012;379:1-10.
33. Luca G, Dirksen MT, Spaulding C et al. Drug-eluting vs bare-metal stents in primary angioplasty: a pooled patient-level meta-analysis of randomized trials. Archives of Internal Medicine 2012;172:1-11.
34. Ormiston JA, Webster MW. Stent thrombosis: has the firestorm been extinguished? Lancet 2012;379:1-2.
35. Ritman EL. Micro-computer tomography: current status and developments. Annual Review of Biomedical Engineering 2004;6:185-208.
36. Oosterwyck H, Duyck J, Sloten J. The use of microfocus computerized tomography as a new technique for characterizing bone tissue around oral implants. J Oral Implantol 2000;26(1):5-12.
37. Langheinrich A, Bohle R, Greschus S. Atherosclerotic lesions at micro ct: feasibility for analysis of coronary artery wall in autopsy specimens. Radiology 2004;231(3):675-681.
38. Rousselle S, Wicks J, Rousselle S et al. Preparation of medical devices for evaluation. Toxicologic Pathology 2008;36:1-5.
39. Komatsu R, Ueda M, Naruko T, Kojima A, Becker AE. Neointimal tissue response at sites of coronary stenting in humans: macroscopic, histological, and immunohistochemical analyses. Circulation 1998;98:224-233.

40. Beusekom HM, Whelan DM, Plas M, Giessen WJ. A practical and rapid method of histological processing for examination of coronary arteries containing metallic stents. Cardiovascular Pathology 1996;5:69-76.
41. Horobin RW. Staining plastic sections. J Microscopy 1983;131:173-186.
42. Rippstein P, Black MK, Boivin M et al. Comparison of processing and sectioning methodologies for arteries containing metallic stents. J Histochem Cytochem 2006;54:673.
43. Daimon T, Kawai K, Kamoto T. Use of a technovit 7200 VLC to facilitate integrated determination of aluminum bylight and electron microscopy. Biotech Histochem 2000;75(1):27-32.
44. Bradshaw SH, Kennedy L, Dexter DF, Veinot JP. A practical method to rapidly dissolve metallic stents. Cardiovascular Pathology 2009;18:127-133.
45. Donath K. Die trenn-dunnschliff-technik zur herstellung histologischer praparate von nicht schneidbaren geweben und materialien. Der Praparator 1995;34:197-206.

VITA

Aaron Roberts received his Bachelor of Science degree in biomedical science from Texas A&M University in 2009. He entered the Master of Science program at Texas A&M University in August. His research interests include cardiovascular disease, the host-tissue response to medical implants, and pathology. He plans to pursue a career in medicine and scientific research.

Mr. Roberts may be reached at the Cardiovascular Pathology Lab at Texas A&M University, 4467 TAMU, College Station, TX 77843. His email is aaronroberts09@gmail.com.